

1 **Comparison of R9.4.1/Kit10 and R10/Kit12 Oxford** 2 **Nanopore flowcells and chemistries in bacterial** 3 **genome reconstruction**

4

5 **1.1 Author names**

6 Nicholas Sanderson^{**1,2} (ORCID: 0000-0001-6370-1961)/Natalia Kapel^{#1,2} (ORCID: 0000-
7 0002-5914-9999), Gillian Rodger^{1,3}, Hermione Webster^{1,2}, Samuel Lipworth^{2,3}, Teresa
8 street^{1,2}, Tim Peto^{1,2,3}, Derrick Crook^{1,2,3} (ORCID: 0000-0002-0590-2850), Nicole
9 Stoesser^{*1,2,3} (ORCID: 0000-0002-4508-7969)

10

11 [#]Contributed equally

12 ^{*}Corresponding/alternative corresponding author

13

14 **1.2 Affiliation**

15 ¹ NIHR Oxford Biomedical Research Centre, University of Oxford, Oxford, UK

16 ² Nuffield Department of Medicine, University of Oxford, Oxford, UK

17 ³ NIHR Health Protection Research Unit in Healthcare Associated Infections and
18 Antimicrobial Resistance at University of Oxford in partnership with Public Health England,
19 Oxford, UK

20

21 Corresponding authors

22 Nicholas Sanderson: nicholas.sanderson@ndm.ox.ac.uk

23 Nicole Stoesser: nicole.stoesser@ndm.ox.ac.uk

24 **1.3 Keyword**

25 Genome sequencing, hybrid assembly, long-read assembly

26 **1.4 Repositories:**

27 Nanopore fast5 and fastq data are available in the ENA under project accession:
28 PRJEB51164.

29

30 Assemblies have been made available at:
31 https://figshare.com/articles/online_resource/q20_comparison_genome_assemblies/19683867

33

34 Code and analysis outputs are available at:
35 https://gitlab.com/ModernisingMedicalMicrobiology/assembly_comparison_analysis/-/tree/main (tagged version v0.5.5).

37

38 **2. Abstract**

39 Complete, accurate, cost-effective, and high-throughput reconstruction of bacterial genomes
40 for large-scale genomic epidemiological studies is currently only possible with hybrid
41 assembly, combining long- (typically using nanopore sequencing) and short-read (Illumina)
42 datasets. Being able to utilise nanopore-only data would be a significant advance. Oxford
43 Nanopore Technologies (ONT) have recently released a new flowcell (R10.4) and chemistry
44 (Kit12), which reportedly generate per-read accuracies rivalling those of Illumina data. To
45 evaluate this, we sequenced DNA extracts from four commonly studied bacterial pathogens,
46 namely *Escherichia coli*, *Klebsiella pneumoniae*, *Pseudomonas aeruginosa* and
47 *Staphylococcus aureus*, using Illumina and ONT's R9.4.1/Kit10, R10.3/Kit12, R10.4/Kit12
48 flowcells/chemistries. We compared raw read accuracy and assembly accuracy for each
49 modality, considering the impact of different nanopore basecalling models, commonly used
50 assemblers, sequencing depth, and the use of duplex versus simplex reads. "Super
51 accuracy" (sup) basecalled R10.4 reads - in particular duplex reads - have high per-read
52 accuracies and could be used to robustly reconstruct bacterial genomes without the use of
53 Illumina data. However, the per-run yield of duplex reads generated in our hands with
54 standard sequencing protocols was low (typically <10%), with substantial implications for
55 cost and throughput if relying on nanopore data only to enable bacterial genome
56 reconstruction. In addition, recovery of small plasmids with the best-performing long-read
57 assembler (Flye) was inconsistent. R10.4/Kit12 combined with sup basecalling holds
58 promise as a singular sequencing technology in the reconstruction of commonly studied
59 bacterial genomes, but hybrid assembly (Illumina+R9.4.1 hac) currently remains the highest
60 throughput, most robust, and cost-effective approach to fully reconstruct these bacterial
61 genomes.

62 **3. Impact statement**

63 Our understanding of microbes has been greatly enhanced by the capacity to evaluate their
64 genetic make-up using a technology known as whole genome sequencing. Sequencers
65 represent microbial genomes as stretches of shorter sequence known as 'reads', which are
66 then assembled using computational algorithms. Different types of sequencing approach
67 have advantages and disadvantages with respect to the accuracy and length of the reads
68 they generate; this in turn affects how reliably genomes can be assembled.

69

70 Currently, to completely reconstruct bacterial genomes in a high-throughput and cost-
71 effective manner, researchers tend to use two different types of sequencing data, namely
72 Illumina (short-read) and nanopore (long-read) data. Illumina data are highly accurate;
73 nanopore data are much longer, and this combination facilitates accurate and complete
74 bacterial genomes in a so-called “hybrid assembly”. However, new developments in
75 nanopore sequencing have reportedly greatly improved the accuracy of nanopore data,
76 hinting at the possibility of requiring only a single sequencing approach for bacterial
77 genomics.

78

79 Here we evaluate these improvements in nanopore sequencing in the reconstruction of four
80 bacterial reference strains, where the true sequence is already known. We show that
81 although these improvements are extremely promising, for high-throughput, low-cost
82 complete reconstruction of bacterial genomes hybrid assembly currently remains the optimal
83 approach.

84 **4. Data summary**

85 **The authors confirm all supporting data, code and protocols have been provided
86 within the article, through supplementary data files, or in publicly accessible
87 repositories.**

88

89 Nanopore fast5 and fastq data are available in the ENA under project accession:
90 PRJEB51164.

91

92 Assemblies have been made available at:
93 [https://figshare.com/articles/online_resource/q20_comparison_genome_assemblies/196838
94 67.](https://figshare.com/articles/online_resource/q20_comparison_genome_assemblies/19683867)

95

96 Code and analysis outputs are available at:
97 [https://gitlab.com/ModernisingMedicalMicrobiology/assembly_comparison_analysis/-
98 /tree/main](https://gitlab.com/ModernisingMedicalMicrobiology/assembly_comparison_analysis/-/tree/main) (tagged version v0.5.5).

99

100 **5. Introduction**

101 Bacterial whole genome sequencing has become a prominent tool in the biological sciences,
102 with wide-ranging applications from epidemiology to diagnostics(1). Important considerations
103 include sequencing throughput, read length (which facilitates complete reconstruction of

104 bacterial chromosomes and plasmids), read accuracy, accessibility and cost. Historically,
105 short-read Illumina sequencing has been the leading high-throughput, high-accuracy
106 technology, but is limited in its capacity to completely reconstruct genomes, particularly in
107 the presence of repetitive sequences. Nanopore sequencing (Oxford Nanopore
108 Technologies [ONT]) has become one of the most widely adopted long-read sequencing
109 approaches, enabled by affordable, small-footprint sequencing platforms, but has been
110 limited to some extent by its accuracy. Combining short and long-read sets from both
111 technologies in the form of hybrid assembly has facilitated cost-effective, highly accurate and
112 scalable genome reconstruction for large bacterial isolate collections(2, 3), such as by
113 multiplexing 96 *E. coli* isolates on a single nanopore flowcell(3). For nanopore sequencing,
114 developments in multiplexing, rapid library preparation and flow cell reuse after washing
115 have streamlined this process(4).

116

117 ONT have undertaken iterative development of their sequencing flowcells and chemistries,
118 releasing the R10.3 (FLO-MIN111) flowcells for consumers in January 2020 and the Kit12
119 (Q20+) chemistry and R10.4 flowcell (FLO-MIN112) in their store in late 2021. The proposed
120 advantages of the R10.4/Kit12 system include: (i) a new motor to facilitate more controlled
121 passage of the nucleic acid template through the sequencing pore thereby avoiding template
122 slippage; (ii) “duplex” read sequencing - where the forward and reverse strand of a single
123 nucleic acid molecule are sequenced in succession to improve accuracy; and (iii) an
124 optimized pore with a longer pore head to better resolve homopolymers.

125

126 These new developments however come with some potential disadvantages. Sequencing
127 yields for the R10.3 flowcells were lower than those using R.9.4.1 flowcells (thought to be
128 due to the slower passage of template through pores)(5). The use of R10 flowcells also
129 currently requires a ligation-based library preparation, which results in longer sequencing
130 turnaround times when compared with rapid transposase-based library preparation kits
131 which can be used with R9.4.1 flowcells. Ligation-based preparations may also miss the
132 capture and sequencing of small plasmids(6). The reported improvements in per-read
133 accuracy with R10/Kit12 are also potentially dependent on the use of super accuracy (sup)
134 basecalling models; however, on the same computing infrastructure sup basecalling takes 2-
135 8x longer than the previous typical approach using high accuracy (hac) basecalling models,
136 which may preclude “on-machine” basecalling in real-time(7).

137

138 Sequencing accuracy can be characterized using several different metrics, including: (i) raw
139 read accuracy (the accuracy achieved when reading a single nucleic acid fragment once)
140 and (ii) assembly accuracy (the capacity to accurately reconstruct complete genomes in
141 terms of structure, sequence identity and coding sequence content). We therefore set out to
142 compare data and assemblies generated by R9.4.1/Kit10 and R10/Kit12 nanopore
143 flowcells/chemistries, comparing these with Illumina-only sequence data and hybrid
144 assembly, and investigating the impact of sup versus hac basecalling and metrics for duplex

145 sequencing reads. We undertook this comparison for four reference bacterial strains
146 reflecting different species, genome sizes, %GC content, plasmid content and plasmid sizes.
147 We also evaluated the impact of sequencing depth on the capacity to reconstruct the
148 reference bacterial genomes, and whether flowcell washing would still enable flow cell reuse
149 with the new flowcells and chemistry.

150 6. Methods

151 *Bacterial isolates and DNA extraction*

152 Four reference bacterial strains were sequenced for this study, namely: *Escherichia coli*
153 CFT073 (Genbank accession: NC_004431.1), *Klebsiella pneumoniae* MGH78578
154 (NC_009648.1-NC_009653.1), *Pseudomonas aeruginosa* PAO1 (NC_002516.2) and
155 *Staphylococcus aureus* MRSA252 (NC_002952.2). Stock cultures were stored at -80°C in
156 nutrient broth supplemented with 10% glycerol. For DNA extraction, stocks were sub-
157 cultured on Columbia blood agar at 37°C overnight.

158

159 Long fragment DNA extraction from sub-cultured strains was performed using the Qiagen
160 Genomic tip 100/G kit (Qiagen). Quality and fragment length assessments were measured
161 with the Qubit fluorometer (ThermoFisher Scientific) and TapeStation (Agilent). The same
162 DNA extract, stored in elution buffer at 4°C was used for all sequencing experiments. DNA
163 concentration and fragment lengths were evaluated longitudinally to ensure that there was
164 minimal obvious degradation (Tables S1-4, Figs.S1-3).

165

166 *Nanopore sequencing*

167 The experimental workflow is shown in Fig.1. For the experiment using the R9.4.1 (FLO-
168 MIN106) flowcell (denoted as R.9.4 throughout), ONT sequencing libraries were prepared by
169 multiplexing DNA extracts from all four isolates using the Rapid Barcoding Sequencing
170 (SQK-RBK004) kit according to the manufacturer's protocol; sequencing was undertaken on
171 a GridION for 48 hours.

172

173 For the experiments using the R10.3 (FLO-MIN111) and R10.4 (FLO-MIN112) flowcells,
174 ONT sequencing libraries were prepared from DNA extracts using the Q20+ Early Access
175 Kit (SQK-Q20EA) ligation-based protocol. During adapter ligation and clean-up the long
176 fragment buffer was used to enrich for DNA fragments >3kb. Each DNA extract was
177 sequenced on a single flowcell. After sequencing the *S. aureus* MRSA252 library, the R10.4
178 (FLO-MIN112) flowcell was washed with the flowcell wash kit (EXP-WSH004) according to
179 the manufacturer's protocol, before reusing the flowcell to sequence the *P. aeruginosa*
180 PAO1 library. For the R10.3 experiments, sequencing was undertaken on a GridION for 48
181 hours; for the unplexed R10.4 experiments sequencing times were terminated prematurely.

182 The flowcell usage strategy and pore counts for each flowcell prior to use are summarised in
183 Table S5.

184

185 Finally, in a separate experiment, the four DNA extracts were also multiplexed on the R10.4
186 (FLO-MIN112) flowcell using the Native Barcoding Kit (SQK-NBD112.24); sequencing was
187 undertaken on a GridION for 48 hours.

188

189 *Illumina sequencing*

190 DNA extracts for all isolates were also sequenced on the Illumina MiSeq, as part of a wider
191 runplexing 20 bacterial extracts. Libraries were constructed following the Illumina DNA Prep
192 protocol, according to the manufacturer's instructions (including standard normalization for
193 libraries ["Protocol A"]). Library DNA concentrations were quantified by Qubit fluorometry and
194 size distributions of libraries determined using the TapeStation, as above. Sequencing was
195 performed using the MiSeq Reagent Micro Kit v2, generating 150 bp paired-end reads.

196

197 *Data processing and bioinformatic methods*

198 R10.4 duplex read pairs were identified and prepared for basecalling using ONT's duplex
199 tools (<https://pypi.org/project/duplex-tools/>; v 0.2.9). R9.4, R10.3, and R10.4 raw nanopore
200 reads were hac basecalled with Guppy (ONT) versions 5.0.12+eb1a981
201 (dna_r9.4.1_450bps_hac.cfg), 5.0.13+bbad529 (res_dna_r103_q20ea_crf_v034.cfg), and
202 5.0.16+b9fcd7b (dna_r10.4_e8.1_hac.cfg) respectively, as recommended by ONT. R9.4,
203 R10.3, R10.4 (all reads) and R10.4 duplex raw nanopore reads were also basecalled using
204 sup models dna_r9.4.1_e8.1_sup.cfg, dna_r10.3_450bps_sup.cfg, dna_r10.4_e8.1_sup.cfg.
205 Basecalled read summary statistics were generated with seqkit stats using '-T' and '-all'
206 flags(8).

207

208 Nanopore reads were subsampled using Rasusa(9) to depths of 10, 20, 30, 40, 50, and 100
209 average coverage. Nanopore reads were assembled with Canu (version 2.2, using
210 maxInputCoverage=100 and otherwise default parameters)(10), or Flye (using the --meta
211 and --nano-hq parameters and otherwise defaults, version 2.9-b1768)(11), both of which are
212 commonly used long-read only assemblers that have been shown to optimize long-read only
213 assembly quality(12). We also explored the impact of polishing nanopore assemblies with 1,
214 2 and 3 rounds of Medaka (default settings; <https://github.com/nanoporetech/medaka>).

215

216 Subsampled nanopore reads were combined with Illumina reads for hybrid assembly using
217 Unicycler (version 0.4.8, default parameters)(13). The SPAdes (version 3.15.3)(14)

218 assemblies generated from Illumina data as part of the Unicycler pipeline were used as the
219 Illumina-only assemblies for comparative evaluations.

220

221 Given the previous discrepancies observed between multiple resequenced assemblies for *E.*
222 *coli* CFT073 and *K. pneumoniae* MGH78578(15), and the genetic and phenotypic
223 differences observed in different laboratory sub-culture stocks of *P. aeruginosa* PAO1(16,
224 17), we generated an Illumina-corrected reference sequence to use as the “gold standard”
225 comparator for this evaluation. Reference genomes for *E. coli* CFT073 (Genbank accession:
226 AE014075.1), *K. pneumoniae* MGH78578 (CP000647.1), *P. aeruginosa* PAO1
227 (NC_002516.2), *S. aureus* MRSA252 (NC_002952.2) and the respective Illumina datasets
228 generated for this study were used as inputs for the SNIPPY pipeline (version 4.6.0)
229 (<https://github.com/tseemann/snippy>); output consensus fasta files represented the new
230 Illumina-corrected reference sequences used in this study.

231

232 Assembled contigs from nanopore, Illumina, and hybrid assemblies were compared against
233 the Illumina-corrected reference sequences using DNAdiff version 1.3(18).

234

235 Assembled contigs from nanopore, Illumina, and hybrid assemblies as well as the Illumina-
236 corrected reference sequences were annotated with Prokka (version 1.14.6)(19), using the
237 corresponding reference GenBank files to ascertain reference proteins using the ‘--proteins’
238 flag.

239

240 Translated amino acid sequences for Prokka annotations in the different test assemblies
241 (Canu, Flye [long-read only], Unicycler [hybrid long-/short-read], SPAdes [short-read only])
242 and Illumina-corrected reference sequences were compared using the script AAcompare.py
243 in the workflow provided (see below for the repository link). This looked for exact amino acid
244 sequence matches (i.e. 100% identity along 100% of the translated protein) between the
245 Illumina-corrected reference and assembled contigs to determine how intact assembled
246 coding sequences were for each assembly method.

247

248 Per read error rates were calculated by mapping the raw reads to the Illumina corrected
249 references sequences using minimap2 (version 2.22-r1101)(18). The percent identity was
250 calculated from the query distance (NM tag) divided by the query length, multiplied by 100,
251 using the bamreadstats.py script provided in the gitlab repository (link below).

252

253 A workflow for this analysis has been written using nextflow(18) and is available on gitlab
254 (https://gitlab.com/ModernisingMedicalMicrobiology/assembly_comparison). Outputs from
255 the analyses are also available in this repository (tagged version v0.5.5).

256

257 *Data visualization*

258 Figures and plots for this manuscript were generated using the ggplot2 and patchwork
259 packages in R (v3.6.2), and Biorender (www.biorender.com).

260 **7. Results**

261 *Sequencing yield and read length distributions*

262 The total data yield after 48 hours of sequencing from the R9.4 flowcell was 11.0Gb (four
263 isolate extracts multiplexed on one sequencing run), compared with 4.0Gb for the R10.4
264 multiplexed run (Table 1, Fig.S4). For the individual R10.3 flowcells a median of
265 8.2Gb/flowcell (IQR: 7.3-8.8Gb) were generated by 48 hours of sequencing, and
266 6.7Gb/flowcell (IQR: 6.6-7.4Gb) for the R10.4 flowcells respectively by 20-30 hours of
267 sequencing (Table 1, Fig.S4). 21.3Mb of data were generated for the extracts from the
268 Illumina runs (Table 1).

269

270 Read length distributions for a subsample of 1000 reads by modality and species are shown
271 in Fig.2; overall, across species for nanopore data the median read length was 3580bp, the
272 maximum read length 388620bp and the minimum read length 77bp. Median read lengths
273 generated using R9.4 were longer (6273bp versus 2930bp for R10.4; two-sample Wilcoxon
274 test, p<0.001, comparison for hac basecalled data; Fig.2A). N50s are represented in Table
275 1; median N50 across species was 19496bp for R9.4.1 hac, 16002bp for R10.3, 20976bp for
276 R10.4 (all) and 16425bp for R10.4 duplex reads.

277

278 *Duplex reads*

279 The median proportion of duplex reads across the four unplexed, single-extract R10.4 runs
280 was 4.5% (3.8% for *E. coli*, 6.1% for *K. pneumoniae*, 4.5% for *P. aeruginosa*, and 4.5% for
281 *S. aureus*). For the multiplexed R10.4 run for each species these proportions were 2.3%,
282 5.4%, 6.0% and 4.7%.

283

284 *Raw read accuracy by sequencing modality and species*

285 Raw read accuracy (% identity when mapped to the reference) for a subsample of 1000
286 reads by sequencing data type/process (i.e. “sequencing modality”) and species was highest
287 (as expected) for Illumina reads (modal accuracy: 100.0%), followed by R10.4 duplex reads

288 basecalled with the sup model (modal accuracy: 99.9%); modal accuracies for all the other
289 approaches were >97.0% (Fig.3). Sup basecalling improved modal accuracy for R10.4
290 reads, but not R10.3 or R9.4 reads; multiplexing had no impact (Fig.3). Median and modal
291 accuracies for each sequencing modality by species are detailed in Table S6.

292

293 In terms of insertions and deletions with respect to the reference, for long-read modalities
294 R10.4 sup called duplex data performed best (Fig.4A, 4B). The median number of insertions
295 observed per read was 0.94, 0.45, 0.37 and 0.0 for R9.4 hac, R10.3 hac and R10.4 sup and
296 R10.4 sup duplex respectively (two-sample Wilcoxon test for each versus R9.4 hac as the
297 reference category; all p<0.001), and for deletions 1.31, 0.73, 0.63 and 0.10 respectively
298 (two-sample Wilcoxon test for each versus R9.4 hac as the reference category; all p<0.001).

299

300 *Assembly accuracy with respect to number of expected contigs in the reference sequences*
301 *and reference sequence size*

302 We evaluated the capacity of each sequencing approach to accurately reconstruct (i) the
303 number of known contigs present in each reference isolate, and (ii) what percentage of the
304 Illumina-corrected reference was covered. All isolates contained single chromosomes only,
305 except the *K. pneumoniae* reference, which contained a chromosome and five plasmids
306 ranging in size from 3478-175879bp (Table 2).

307

308 Approaches using all the data and Unicycler or Flye largely generated single chromosomal
309 contigs, except those using R10.4 duplex reads only, particularly for multiplexed extracts,
310 likely because these reads were insufficient to cover the whole genome (Table 2; Fig.S5A).
311 Illumina-only assemblies generated much larger numbers of contigs as expected (Table 2).
312 Using all the data, single *K. pneumoniae* plasmid contigs were mostly obtained using any of
313 the long-read data and Flye, or hybrid assembly with Unicycler (Table 2, Fig.S5B). Using all
314 the data, Flye long-read only assemblies largely all missed the two smallest plasmids (Table
315 2, Fig.S5B).

316

317 Sub-sampling the data to 10x, 20x, 30x, 40x, 50x or 100x depth had variable effect - for the
318 most part single chromosomal contigs were assembled using long-reads only with >20x
319 depth; Unicycler could mostly be used with 10x long-read depth (Fig.S5A). The same effect
320 was seen for plasmids, except Flye struggled to reliably assemble the two largest plasmids
321 into single contigs with lower sequencing depths (Fig.S5B). Canu assemblies failed with 10x
322 sub-sampling, as expected given the default cut-offs.

323

324 For chromosomes, Canu long-read only assemblies tended to over-assemble structures (i.e.
325 reference coverage >100%, Fig.5A) whilst Illumina-only assemblies under-assembled

326 structures. Reference coverage % for Unicycler hybrid (R9.4+Illumina) was largely
327 unaffected by sub-sampling the data to 10x, 20x, 30x, 40x, 50x or 100x (Fig.5A). For
328 plasmids, Canu assembly again largely over-assembled the structures; Unicycler hybrid
329 (R9.4+Illumina) assembly was the only approach which consistently assembled all plasmids
330 at near 100% reference coverage across all sub-sampling depths (Fig.5B).

331

332 *Assembly accuracy with respect to insertions, deletions and nucleotide-level mismatches*

333 For each sequencing and assembly modality the number of indels and nucleotide-level
334 mismatches (SNPs) were evaluated by species (Figs.6A, 6B) and overall (Table S7). The
335 impact of sub-sampling and relevance of long-read sequencing depth was also considered
336 (Fig.7).

337

338 Overall, SPAdes assemblies had the fewest indels (0.02 indels/100kb), followed by Medaka-
339 polished Flye-assembled R10.4 sup basecalled/duplex reads (0.18 indels/100kb), Medaka-polished
340 Flye-assembled R10.4 sup basecalled data (0.41 indels/100kb), Medaka-polished
341 Flye-assembled R10.3 hac basecalled data (for 3 rounds of polishing: 0.44 indels/100kb)
342 and Unicycler assemblies (0.56 indels/100kb) (Table S7). There were apparent species-
343 specific differences, with the *E. coli* reference proving the most challenging to assemble
344 accurately (Fig.6A). The improvements in the indel error rates of R9.4 or R10.4 Flye
345 assemblies polished with 2 or 3 rounds of Medaka versus 1 round were negligible; however,
346 additional rounds of polishing improved indel errors in R10.3 hac basecalled assemblies
347 (Fig.6A, Fig.S6, Table S7).

348

349 Similar trends were observed overall for SNPs, with the lowest error rates (0.21 SNPs/100
350 kb of sequence) observed for multiply-Medaka-polished Flye-assembled R10.3 hac
351 basecalled data, or singly-Medaka-polished Flye assembled R10.4 sup basecalled/duplexed
352 data (0.21 SNPs/100kb of sequence) (Fig.6B, Table S7). SNP error rates for Unicycler
353 assemblies however were higher than for the other optimised assembly modalities (4.38
354 SNPs/100kb) (Tables S7). Polishing Flye assemblies with Medaka improved SNP error rates
355 over unpolished assemblies, but there were no obvious benefits of multiple rounds of
356 polishing (Fig.6B, Fig.S6). Again, species-specific differences were observed, with the *E. coli*
357 reference the most challenging to assemble (Fig.6B).

358

359 Error rates for Unicycler assemblies were largely consistent at all long-read sequencing
360 depths from 10X to up to strategies using all the data; error rates for long-read-only
361 assemblies were optimised when coverage was $\geq 20X$ (Fig.7).

362

363 *Assembly accuracy with respect to coding sequence content*

364 Coding sequence content was most accurately recovered using Flye-assembled sup
365 basecalled R10.4 duplex data and hybrid assembly (Fig.8; missing between 9-32 (~0.25-
366 0.75%) of coding sequences across species). Long-read only assembly with R9.4 data
367 missed up to 10-15% of coding sequences (data not plotted in Fig.8). Notably, the duplex
368 datasets from the unplexed 10.4 runs were used, as from multiplexed runs the duplex yields
369 were insufficient to facilitate assembly in most cases (Table 2).

370

371 8. Discussion

372 In this pragmatic study evaluating the impact of different nanopore sequencing flowcells and
373 chemistries on the capacity to fully reconstruct genomes of four commonly studied bacteria,
374 we have shown that sup basecalled R10.4/Kit12 data and sup called duplex data have read-
375 and assembly-level accuracies that would enable these to be effectively used for the
376 reconstruction of bacterial genomes without requiring Illumina data to generate hybrids.
377 However, hybrid assembly (Illumina+9.4.1 hac data) remains the most robust approach in
378 terms of contig (both chromosomes and plasmids) and CDS recovery without over-
379 assembly, and facilitates the multiplexing of large numbers of isolates per flowcell, given that
380 in this and at least one other study(3), $\leq 10x$ long-read depth is required for the accurate
381 reconstruction of chromosomes and plasmids by combining R9.4.1 and Illumina data using
382 Unicycler. Highly accurate long-read only assembly and genome reconstructions was
383 optimized by generating duplex reads, which in our hands made up a small proportion of the
384 output (<10%); as such, it would come at a significant cost per isolate as a result of being
385 able to only generate data for 1-2 isolates per flowcell. Very approximate costs per genome
386 therefore for hybrid assembly versus duplex/long-read-only assembly would be £50-
387 70/genome versus £300-600/genome.

388

389 Although barcoding up to 96 isolates has recently been enabled for the R10.4/Kit12
390 combination, the data yields per flowcell (~4Gb) would likely preclude viable assembly for 96
391 *E. coli* isolates with a typical genome size of ~5Mb (would give <8x coverage). There is also
392 a current requirement to use a ligation-based library preparation, which lengthens the
393 processing time, and may impact on plasmid recovery(6). We observed issues with
394 recovering small plasmids (<5kb) using Flye in this study although both of these small
395 plasmids could be reliably recovered in Canu assemblies; consistent with this a previous
396 evaluation has shown that 8-15% of small plasmids are not recovered using these long-read-
397 only assemblers(12). Similarly, as shown in this study and in other work(12), the basic Canu
398 workflow 'over-assembles' the data, and contigs require trimming of overlaps in order to
399 recreate accurate, single, circularized structures. We observed some apparent species-
400 specific differences, suggesting that assemblers are more challenged in accurately
401 reconstructing certain genomes; these differences, as well as differences related to genome
402 length and the impact on long-read sequencing depth may be important to consider in study
403 design.

404

405 There are currently few other published studies on the performance of R10.4/Kit12 for
406 bacterial analyses. We found only one preprint investigating its use on a mock microbial
407 community (7 bacterial species and 1 fungal species) which found similar modal accuracy
408 scores of 99% using sup basecalling, and a requirement of 40x to be able to reliably
409 assemble a genome(20). Their hypothesis was that improved read accuracies were due to
410 an improved ability to call homopolymers, which we did not investigate in this manuscript. It
411 was unclear what proportion of reads they characterized as duplex reads.

412

413 There are several limitations of our study. We have not exhaustively investigated all possible
414 approaches to genome assembly, but rather taken a pragmatic approach in assembling the
415 data with several commonly used assemblers, without additional bespoke management or
416 combination of workflows; the data are however available for other researchers to trial
417 different approaches. We had low duplex read yields compared with those reported by ONT
418 (up to 30-40% per flowcell); further optimization is needed to see if these can be achieved.
419 We have investigated only a limited number of isolates and plasmids, but these represent a
420 range of %GC and sizes, and are likely to reflect genetic content more widely in other
421 species; we have not generated replicate datasets. Similarly, because we only investigated
422 one isolate per species, it may be that the differences observed are not generalisable or are
423 strain and not species-specific; this would be interesting future work. Improvements and
424 upgrades to nanopore flowcells, chemistries and basecallers occur regularly and nanopore
425 will be releasing the R10.4.1 flowcell and kit14 chemistries later in 2022 which may further
426 optimise the quality of long-read only outputs.

427

428 In summary, the combination of R10.4/Kit12 flowcells/chemistries look very promising for
429 highly accurate, long-read only bacterial genome assembly; however, this requires superior
430 accuracy basecalling, and is optimised by the generation of duplex reads, which currently
431 make up only a small proportion of sequencing yield. In addition, for large-scale projects to
432 fully reconstruct 100s-1000s of bacterial isolates, hybrid assembly, multiplexing and the use
433 of flowcells/chemistries that support rapid barcoding are currently better suited for higher
434 throughput and are more cost-effective per reconstructed genome. The optimal strategy in
435 any given context will depend on the specific use case and resources available, and may
436 evolve rapidly over short timescales.

437 **9. Author statements**

438 **9.1 Authors and contributors**

439 NK, NSa, DWC and NS designed the study. NK and GR performed the laboratory
440 experiments and sequencing. NSa performed the bioinformatics analysis. NSt generated the
441 data visualisations. NSt, NSa and NK wrote the first draft. All authors reviewed and approved
442 the final draft.

443

444 **9.2 Conflicts of interest**

445 Oxford Nanopore Technologies supplied the R10.3 and R10.4 flowcells free of charge for
446 this study. They were also involved in discussions regarding which data processing
447 approaches to use to optimise basecalling and assembly outputs; however, they did not
448 impact on the presentation of any of the results.

449

450 **9.3 Funding information**

451 This study was funded by the National Institute for Health Research (NIHR) Health
452 Protection Research Unit in Healthcare Associated Infections and Antimicrobial Resistance
453 (NIHR200915), a partnership between the UK Health Security Agency (UKHSA) and the
454 University of Oxford, and was supported by the NIHR Oxford Biomedical Research Centre
455 (BRC). The computational aspects of this research were funded from the NIHR Oxford BRC
456 with additional support from the Wellcome Trust Core Award Grant Number 203141/Z/16/Z.
457 The views expressed are those of the author(s) and not necessarily those of the NHS, NIHR,
458 UKHSA or the Department of Health and Social Care. For the purpose of open access, the
459 author has applied a Creative Commons Attribution (CC BY) licence to any Author Accepted
460 Manuscript version arising. NS is an NIHR Oxford BRC Senior Research Fellow and an
461 Oxford Martin Fellow.

462

463 **9.4 Ethical approval**

464 Not applicable.

465 **9.5 Consent for publication**

466 Not applicable.

467 **9.6 Acknowledgements**

468 We are grateful to Dr Celiq Souque and Prof Craig Maclean at the Department of Zoology,
469 University of Oxford, for supplying the *Pseudomonas aeruginosa* PAO1 strain. We are also
470 grateful for feedback from the Twitter community following the release of this manuscript as
471 a preprint.

472

473 **10. References**

- 474 1. Van Goethem N, Descamps T, Devleesschauwer B, Roosens NHC, Boon NAM, Van
475 Oyen H, et al. Status and potential of bacterial genomics for public health practice: a scoping
476 review. *Implementation science : IS.* 2019;14(1):79.
- 477 2. Shaw LP, Chau KK, Kavanagh J, AbuOun M, Stubberfield E, Gweon HS, et al. Niche
478 and local geography shape the pangenome of wastewater- and livestock-associated
479 Enterobacteriaceae. *Science advances.* 2021;7(15).

480 3. Arredondo-Alonso S, Pöntinen AK, Cléon F, Gladstone RA, Schürch AC, Johnsen
481 PJ, et al. A high-throughput multiplexing and selection strategy to complete bacterial
482 genomes. *GigaScience*. 2021;10(12).

483 4. Lipworth S, Pickford H, Sanderson N, Chau KK, Kavanagh J, Barker L, et al.
484 Optimized use of Oxford Nanopore flowcells for hybrid assemblies. *Microb Genom*.
485 2020;6(11).

486 5. Oxford Nanopore Technologies. <https://nanoporetech.com/about-us/news/r103-newest-nanopore-high-accuracy-nanopore-sequencing-now-available-store>; last accessed:
487 07/Apr/2022.

488 6. Wick RR, Judd LM, Wyres KL, Holt KE. Recovery of small plasmid sequences via
489 Oxford Nanopore sequencing. *Microb Genom*. 2021;7(8).

490 7. Benton M. 2021. Nanopore Guppy GPU basecalling on Windows using
491 WSL2`https://hackmd.io/@Miles/rkYKDHPsO`. Blog post, last accessed: 07/Apr/2022.

492 8. Shen W, Le S, Li Y, Hu F. SeqKit: A Cross-Platform and Ultrafast Toolkit for
493 FASTA/Q File Manipulation. *PLoS One*. 2016;11(10):e0163962.

494 9. Hall MB. Rasusa: Randomly subsample sequencing reads to a specified coverage.
495 The Journal of Open Source Software.

496 10. Koren S, Walenz BP, Berlin K, Miller JR, Bergman NH, Phillippy AM. Canu: scalable
497 and accurate long-read assembly via adaptive k-mer weighting and repeat separation.
498 *Genome Res*. 2017;27(5):722-36.

499 11. Kolmogorov M, Yuan J, Lin Y, Pevzner PA. Assembly of long, error-prone reads
500 using repeat graphs. *Nature biotechnology*. 2019;37(5):540-6.

501 12. Wick RR, Holt KE. Benchmarking of long-read assemblers for prokaryote whole
502 genome sequencing. *F1000Research*. 2019;8:2138.

503 13. Wick RR, Judd LM, Gorrie CL, Holt KE. Unicycler: Resolving bacterial genome
504 assemblies from short and long sequencing reads. *PLoS Comput Biol*.
505 2017;13(6):e1005595.

506 14. Prjibelski A, Antipov D, Meleshko D, Lapidus A, Korobeynikov A. Using SPAdes De
507 Novo Assembler. *Curr Protoc Bioinformatics*. 2020;70(1):e102.

508 15. De Maio N, Shaw LP, Hubbard A, George S, Sanderson ND, Swann J, et al.
509 Comparison of long-read sequencing technologies in the hybrid assembly of complex
510 bacterial genomes. *Microb Genom*. 2019.

511 16. Klockgether J, Munder A, Neugebauer J, Davenport CF, Stanke F, Larbig KD, et al.
512 Genome diversity of *Pseudomonas aeruginosa* PAO1 laboratory strains. *J Bacteriol*.
513 2010;192(4):1113-21.

514

515 17. Chandler CE, Horspool AM, Hill PJ, Wozniak DJ, Schertzer JW, Rasko DA, et al.
516 Genomic and Phenotypic Diversity among Ten Laboratory Isolates of *Pseudomonas*
517 *aeruginosa* PAO1. *J Bacteriol.* 2019;201(5).

518 18. Kurtz S, Phillippy A, Delcher AL, Smoot M, Shumway M, Antonescu C, et al.
519 Versatile and open software for comparing large genomes. *Genome Biol.* 2004;5(2):R12.

520 19. Seemann T. Prokka: rapid prokaryotic genome annotation. *Bioinformatics.*
521 2014;30(14):2068-9.

522 20. Sereika MK, R.H.; Karst, S.M.; Michaelsen, T.Y.; Soresnes, E.A.; Wollenberg, R.D.;
523 Albertsen, M. Oxford Nanopore R10.4 long-read sequencing enables near-perfect bacterial
524 genomes from pure cultures and metagenomes without short-read or reference polishing.
525 *BioRxiv.*

526

527 **11. Figures and tables**

528 **Table 1. Sequencing read statistics by sequencing modality and bacterial species.**

529 Note for R.9.4/Kit10 four isolates were plexed and the total data output is a composite of the
530 individual outputs; for the R10.3/Kit12 and R10.4/Kit12 evaluations each isolate extract was
531 initially run separately. The same flowcell was washed and then re-used for the R10.4
532 evaluation for the *S. aureus* and then *P. aeruginosa* isolates. Finally, the four DNA extracts
533 were also multiplexed on a single R10.4/Kit12 run.

534

| Species | Sequencing modality/sub-group | Total reads | Total bases | N50 | Percentage of reads with a phred score of ≥ 20 |
|----------------|---|-------------|-------------|-------|---|
| <i>E. coli</i> | Illumina | 3801912 | 574088712 | 151 | 97.93 |
| | R9.4 (multiplexed run) | 353317 | 2364469570 | 11705 | 67.1 |
| | R9.4 (multiplexed run; sup called) | 339077 | 2242222750 | 11535 | 70.03 |
| | R10.3 (single extract/run) | 1073327 | 5964466078 | 9852 | 79.05 |
| | R10.3 (single extract/run; sup called) | 1072758 | 5936766616 | 9827 | 73.5 |
| | R10.4 (single extract/run ; overall) | 1174227 | 6124985330 | 10507 | 66.2 |
| | R10.4 (single extract/run; sup called) | 1167782 | 6131556595 | 10562 | 79.09 |
| | R10.4 (single extract/run; sup called and duplex reads) | 52171 | 229801689 | 7274 | 98.21 |
| | R10.4 (multiplexed) | 286239 | 671853044 | 5327 | 72.62 |

| | run) | | | | |
|----------------------|---|---------|------------|-------|-------|
| | R10.4 (multiplexed run; sup called and duplex reads) | 6447 | 10999797 | 3403 | 98.06 |
| <i>K. pneumoniae</i> | Illumina | 3202356 | 483555756 | 151 | 97.45 |
| | R9.4 (multiplexed run) | 377192 | 3646791131 | 17396 | 65.23 |
| | R9.4 (multiplexed run; sup called) | 361657 | 3458646526 | 17157 | 68.59 |
| | R10.3 (single extract/run) | 789562 | 7772922913 | 19228 | 77.29 |
| | R10.3 (single extract/run; sup called) | 774119 | 7658992847 | 19124 | 70.24 |
| | R10.4 (single extract/run ; overall) | 869853 | 7481444246 | 18612 | 65.83 |
| | R10.4 (single extract/run; sup called) | 865400 | 7495921601 | 18697 | 79.79 |
| | R10.4 (single extract/run; sup called and duplex reads) | 54177 | 452672411 | 16484 | 98.62 |
| | R10.4 (multiplexed run) | 224555 | 1667146081 | 15525 | 72.1 |
| | R10.4 (multiplexed run; sup called and duplex reads) | 12114 | 95832563 | 15245 | 98.82 |
| <i>P. aeruginosa</i> | Illumina | 5299866 | 800279766 | 151 | 97.25 |

| | | | | | |
|------------------|--|---------|------------|-------|-------|
| | | | | | |
| | R9.4 (multiplexed run) | 361977 | 4302642519 | 21597 | 66.49 |
| | R9.4 (multiplexed run; sup called) | 351155 | 4138688286 | 21342 | 71.55 |
| | R10.3 (single extract/run) | 1024134 | 8524041501 | 17666 | 81.81 |
| | R10.3 (single extract/run; sup called) | 1017748 | 8528041241 | 17683 | 76.05 |
| | R10.4 (single extract/run ; overall) | 556000 | 5851279980 | 24126 | 67.35 |
| | R10.4 (single extract/run; sup called) | 638801 | 6378501910 | 23860 | 82.24 |
| | R10.4 (single extract/run; sup called and duplex reads) | 22859 | 261812617 | 21432 | 98.58 |
| | R10.4 (multiplexed run) | 208693 | 1412016443 | 14627 | 73.91 |
| | R10.4 (multiplexed run; sup called and duplex reads) | 12468 | 93018395 | 14095 | 98.83 |
| <i>S. aureus</i> | Illumina | 9033160 | 1364007160 | 151 | 98.98 |
| | R9.4 (multiplexed run) | 40194 | 725665757 | 33599 | 72.67 |
| | R9.4 (multiplexed run; sup called) | 39155 | 699249807 | 33066 | 75.51 |

| | | | | | |
|--|---|---------|------------|-------|-------|
| | R10.3 (single extract/run) | 1625258 | 9724520340 | 14338 | 82.06 |
| | R10.3 (single extract/run; sup called) | 1645001 | 9819093990 | 14337 | 78.84 |
| | R10.4 (single extract/run ; overall) | 950361 | 7371346901 | 23339 | 74.06 |
| | R10.4 (single extract/run; sup called) | 945421 | 7382123466 | 23446 | 84.24 |
| | R10.4 (single extract/run; sup called and duplex reads) | 47087 | 334258567 | 16366 | 98.8 |
| | R10.4 (multiplexed run) | 80512 | 287957484 | 14301 | 80.04 |
| | R10.4 (multiplexed run; sup called and duplex reads) | 3753 | 12755562 | 10232 | 99.08 |

536 **Table 2. Number of unique contigs by sequencing modality and bacterial species.** Using the complete data available (i.e. no
 537 subsampling). The first number in each cell represents the number of contigs assembled and matching to the Illumina-corrected reference
 538 using dnadiff, the total number of contigs assembled is shown in curved brackets, and the proportion of the reference chromosomal contig
 539 covered in square brackets. For *E. coli*, *P. aeruginosa*, *S. aureus* the total number of expected contigs is 1, for *K. pneumoniae* 1 chromosome +
 540 5 plasmids. Orange shading shows absent contigs, and/or incomplete assembly (n >1 contig matching to reference), and/or extra contigs not
 541 matching to reference. Green shaded cells denote complete singular contigs which reflect the reference DNA content at 100+/-1%. “-“ denotes
 542 no relevant contig assembled.

543

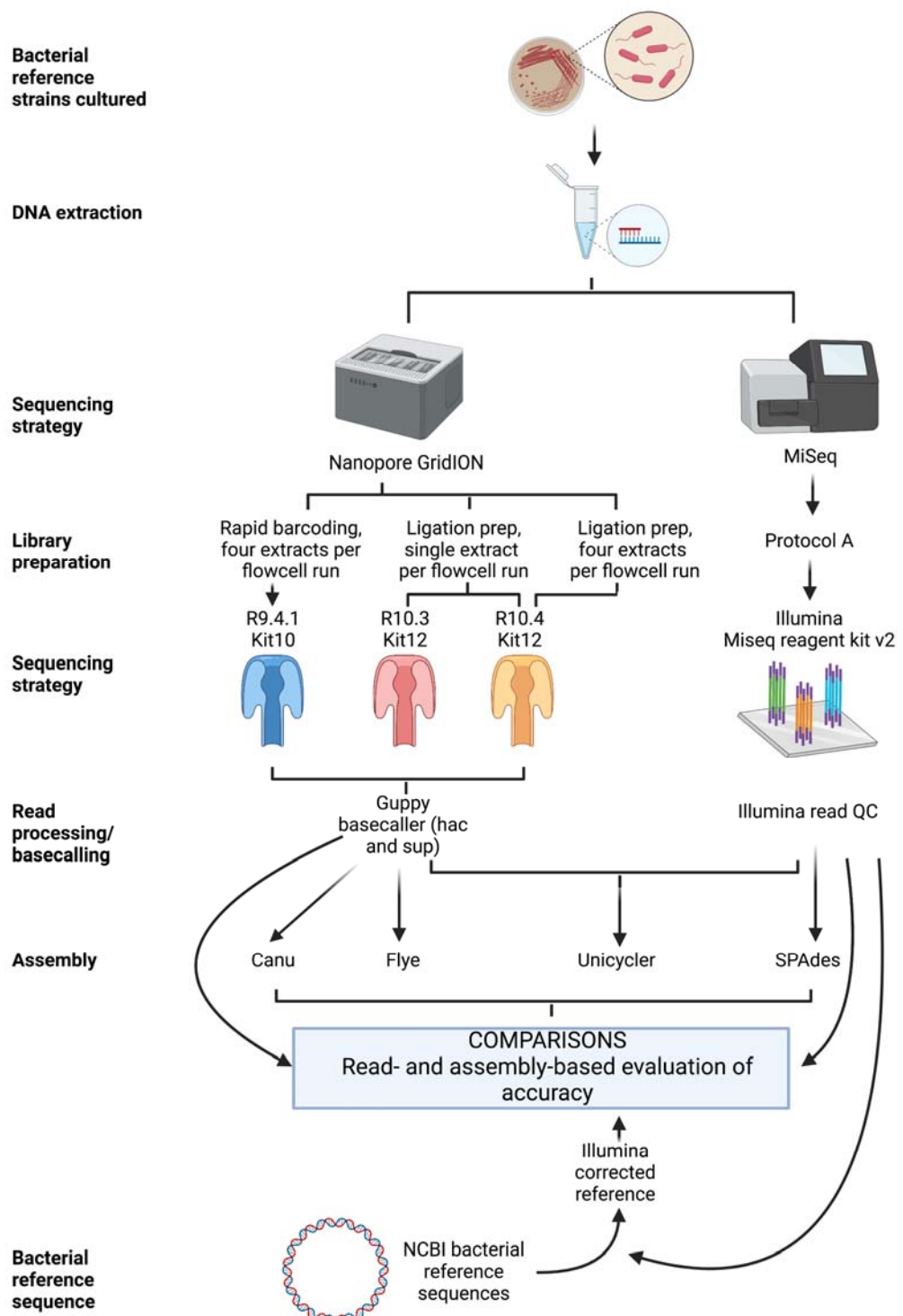
| Sequencing modality | Assembler | Plexed Y/N | <i>E. coli</i> , chromosome (1) 5231428bp | <i>P. aeruginosa</i> , chromosome (1) 51% GC | <i>S. aureus</i> , chromosome (1) 6264404bp | <i>K. pneumoniae</i> , chromosome (1) 32.8%GC | <i>K. pneumoniae</i> , pKPN3 plasmid (1) 5315120bp | <i>K. pneumoniae</i> , pKPN4 plasmid (1) 51.7%GC | <i>K. pneumoniae</i> , pKPN5 (plasmid (1) 53.4%GC | <i>K. pneumoniae</i> , pKPN6 (plasmid (1) 53.8%GC | <i>K. pneumoniae</i> , pKPN7 (plasmid (1) 41.4%GC |
|---------------------|-----------|------------|--|---|--|--|---|---|--|--|--|
| Illumina | SPAdes | Y | 226 (326) [98.64%] | 115 (152) [99.72%] | 86 (150) [98.42%] | 117 (312) [98.9%] | 41 [79.7%] | 45 [100.72%] | 22 [82.49%] | 1 [102.82%] | 1 [103.45%] |
| R9.4.1 hac+Illumina | Unicycler | Y | 1 (1) [100.09%] | 1 (1) [100.49%] | 1 (1) [100.69%] | 1 (7) [100.1%] | 1 [100%] | 1 [100%] | 1 [100%] | 2 [100%] | 1 [96.15%] |
| R9.4.1 hac | Canu | Y | 1 (1) [100.59%] | 1 (1) [101.29%] | 1 (1) [103.18%] | 1 (24) [100.72%] | 1 [131.55%] | 1 [172.51%] | 1 [100%] | 2 [133.5%] | 1 [100%] |

| | | | | | | | | | | | |
|------------------|------|---|---------------------|--------------------|---------------------|---------------------|----------------|----------------|----------------|----------------|----------------|
| R9.4.1 sup | Canu | Y | 1 (1) [100.65%] | 1 (1) [101.18%] | 1 (1) [102.43%] | 1 (7) [100.96%] | 1 [129.41%] | 1 [100%] | 1 [125.07%] | 1 [100%] | 1 [100%] |
| R10.3 hac | Canu | N | 1 (6) [100.49%] | 1 (2) [101.19%] | 1 (3) [102.78%] | 1 (8) [100.72%] | 1 [100%] | 1 [100%] | 1 [100%] | 1 [100%] | 1 [100%] |
| R10.3 sup | Canu | N | 1 (2) [100.6%] | 1 (3) [101.13%] | 1 (3) [102.85] | 1 (8) [100.74%] | 1 [100%] | 1 [138.13%] | 1 [143.94%] | 1 [192.58%] | 1 [100%] |
| R10.4 hac | Canu | N | 1 (6) [100.62%] | 1 (1) [101.06%] | 1 (2) [103.6%] | 1 (8) [100.8%] | 1 [127.89%] | 1 [141.81%] | 1 [147.6%] | 1 [100%] | 1 [112.85%] |
| R10.4 sup | Canu | N | 1 (3) [100.61%] | 1 (2) [100.1%] | 1 (2) [102.33%] | 1 (7) [100%] | 1 [100.94%] | 1 [100%] | 1 [145.43%] | 1 [100%] | 1 [100%] |
| R10.4 sup duplex | Canu | N | 4 (42) [100.12%] | 1 (14) [101.5%] | 1 (29) [101.72%] | 1 (41) [100.1%] | 1 [100%] | 3 [130.98%] | 1 [149.19%] | 1 [100%] | 1 [100%] |
| R10.4 hac | Canu | Y | 1 (2) [100.42%] | 1 (1) [100.87%] | 1 (1) [102.01%] | 1 (7) [100.82%] | 1 [124.01%] | 1 [100%] | 1 [142.89%] | 1 [100%] | 1 [100%] |
| R10.4 sup | Canu | Y | 1 (1) [100.48%] | 1 (1) [100.17%] | 1 (1) [102.29%] | 1 (12) [100.61%] | 1 [117.3%] | 2 [134.06%] | 1 [137.68%] | 1 [100%] | 1 [100%] |
| R10.4 sup duplex | Canu | Y | -* | 23 (25) [99.2%] | -* | 15 (25) [99.2%] | 1 [80.39%] | 2 [97.73%] | 1 [112.86%] | 1 [94.01%] | 1 [100%] |
| R9.4.1 hac | Flye | Y | 1 (1) [100.09%] | 1 (1) [100.14%] | 1 (1) [100.7%] | 1 (4) [100.11%] | 1 [75.7%] | 1 [103.68%] | 1 [100%] | - | - |
| R9.4.1 sup | Flye | Y | 1 (1) [100.09%] | 1 (1) [100.47%] | 1 (1) [100%] | 1 (5) [100.1%] | 1 [100%] | 1 [99.99%] | 1 [100%] | - | - |

| | | | | | | | | | | | |
|------------------|------|---|--------------------|--------------------|---------------------|--------------------|------------|----------------|----------------|---|----------|
| R10.3 hac | Flye | N | 1 (1) [100.10%] | 1 (1) [100.44%] | 1 (1) [100.69%] | 1 (4) [100.1%] | 1 [95.83%] | 1 [73.13%] | 1 [100%] | - | - |
| R10.3 sup | Flye | N | 1 (1) [100.09%] | 1 (1) [100.44%] | 1 (1) [100.69%] | 1 (4) [100.1%] | 1 [100%] | 1 [100%] | 1 [100%] | - | - |
| R10.4 hac | Flye | N | 1 (1) [100.10%] | 1 (1) [100.11%] | 1 (1) [100.69%] | 1 (4) [100.1%] | 1 [100%] | 1 [100%] | 1 [100%] | - | - |
| R10.4 sup | Flye | N | 1 (1) [100.09%] | 1 (1) [100.4%] | 1 (1) [100.69%] | 1 (5) [100.1%] | 1 [100%] | 1 [98.92%] | 1 [99.99%] | - | - |
| R10.4 sup duplex | Flye | N | 1 (3) [100.10%] | 1 (1) [100.8%] | 1 (2) [100.69%] | 1 (7) [100.21%] | 1 [94.27%] | 1 [102.93%] | 1 [101.54%] | - | 1 [100%] |
| R10.4 hac | Flye | Y | 1 (1) [100.10%] | 1 (1) [100.16%] | 1 (1) [100.69%] | 1 (5) [100.1%] | 1 [100%] | 1 [100%] | 1 [100%] | - | - |
| R10.4 sup | Flye | Y | 1 (1) [100.00%] | 1 (1) [100.48%] | 1 (1) [100.69%] | 1 (5) [100.11%] | 1 [100%] | 1 [100%] | 1 [100%] | - | - |
| R10.4 sup duplex | Flye | Y | 37 (38) [8.47%] | 1 (5) [100.48%] | 25 (25) [83.64%] | 1 (4) [100.4%] | 1 [84.71%] | 1 [105.27%] | 1 [100%] | - | - |

545 **Figure 1. Experimental workflow**

546



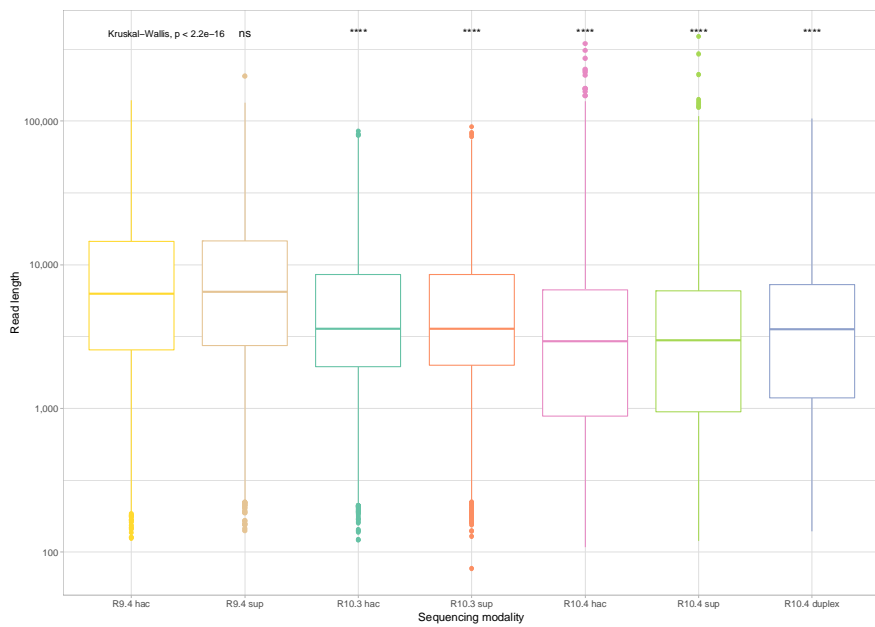
547

548 **Figure 2. Read length distributions by (A) modality and (B) by modality and species.**

549 Boxplots reflect median (central line) and IQR (box hinges) values, whiskers the smallest
550 and largest values 1.5*IQR, and dots the outlying points beyond these ranges. Note the y-
551 axis is a log-scale. Median differences in read length were significant across the whole
552 dataset (Kruskal-wallis, $p < 0.001$); other significance values represent comparisons with the
553 average read length for R9.4 hac as the reference category (“ns” - not significant, “****” -
554 $p < 0.001$).

555

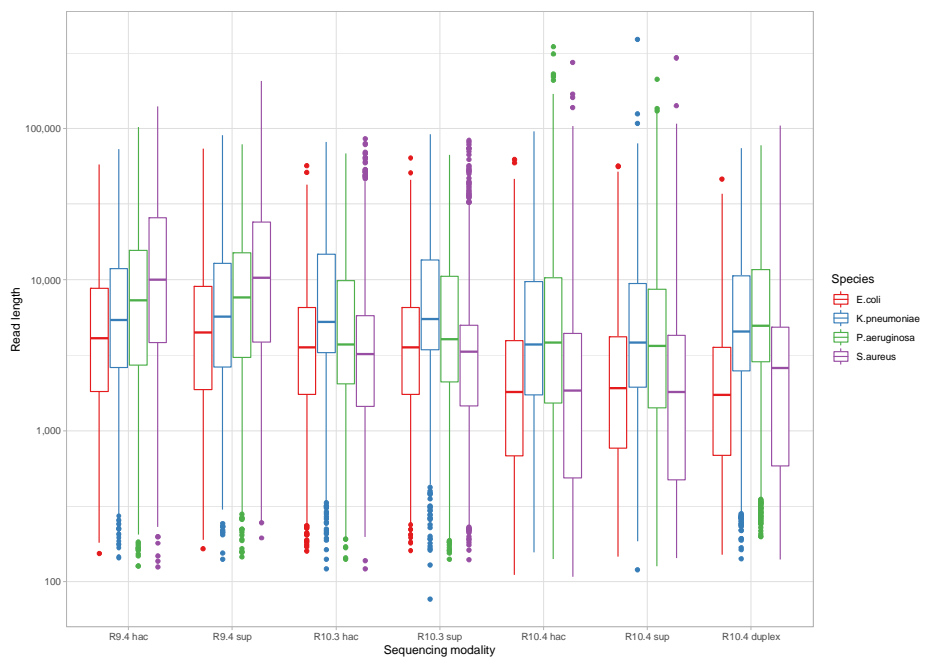
556 (A)



557

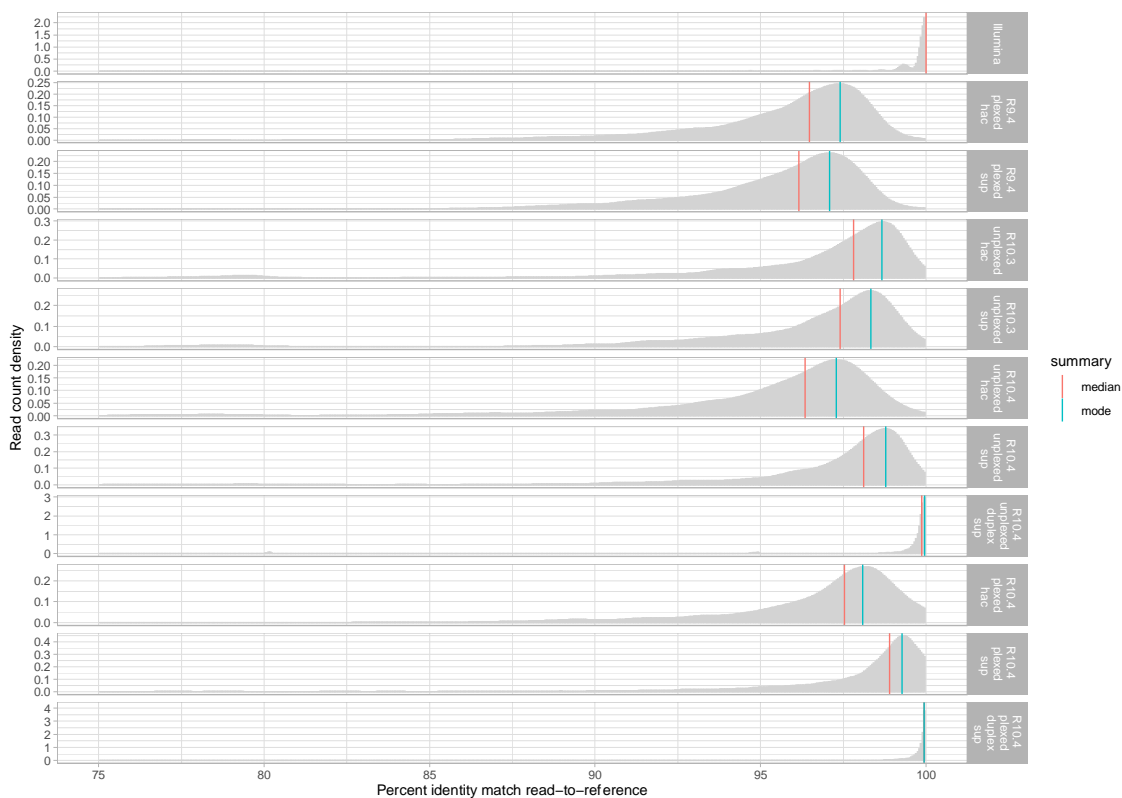
558

559 (B)



561 **Figure 3. Median and modal raw read accuracy (% identity when reads are mapped to**
562 **the Illumina-corrected reference) for each of the major nanopore sequencing**
563 **sequencing modalities, flowcells/kit and basecalling combinations.** Reads matching to
564 the reference with <75% identity have been excluded. Complete details summarising all
565 accuracies across all modality, flowcell/kit and basecalling combinations, and stratified by
566 species are represented in Supplementary Table S6.

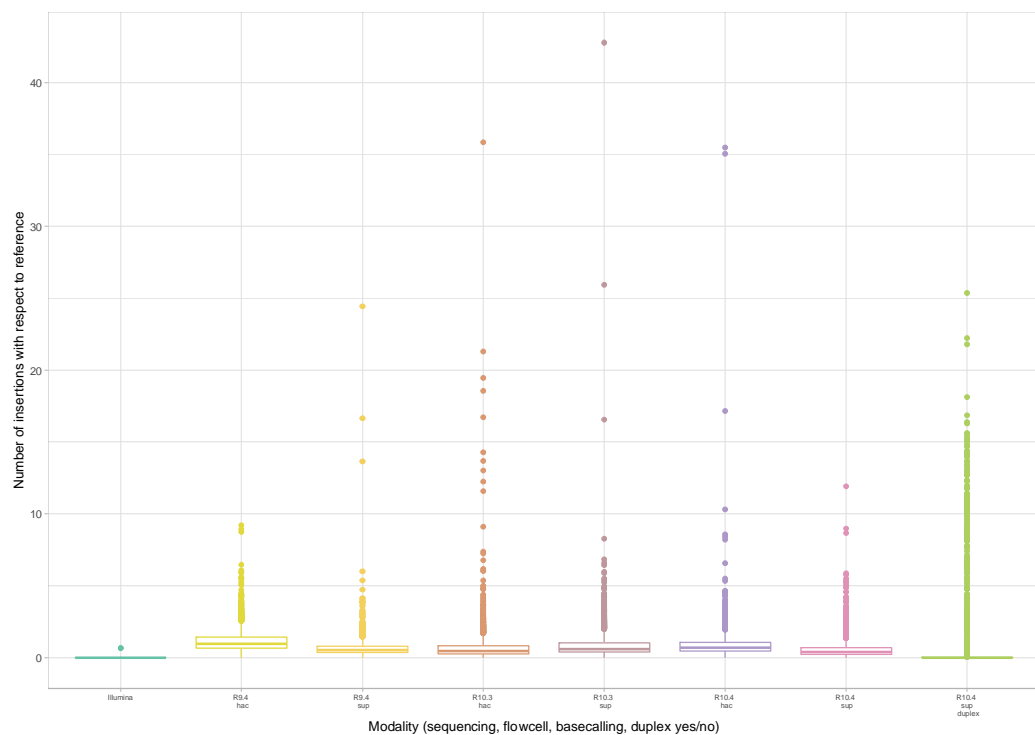
567



568

569 **Figure 4. Number of insertions (panel A) and deletions (panel B) amongst reads**
570 **mapped to the Illumina-corrected reference for all sequencing modalities.**

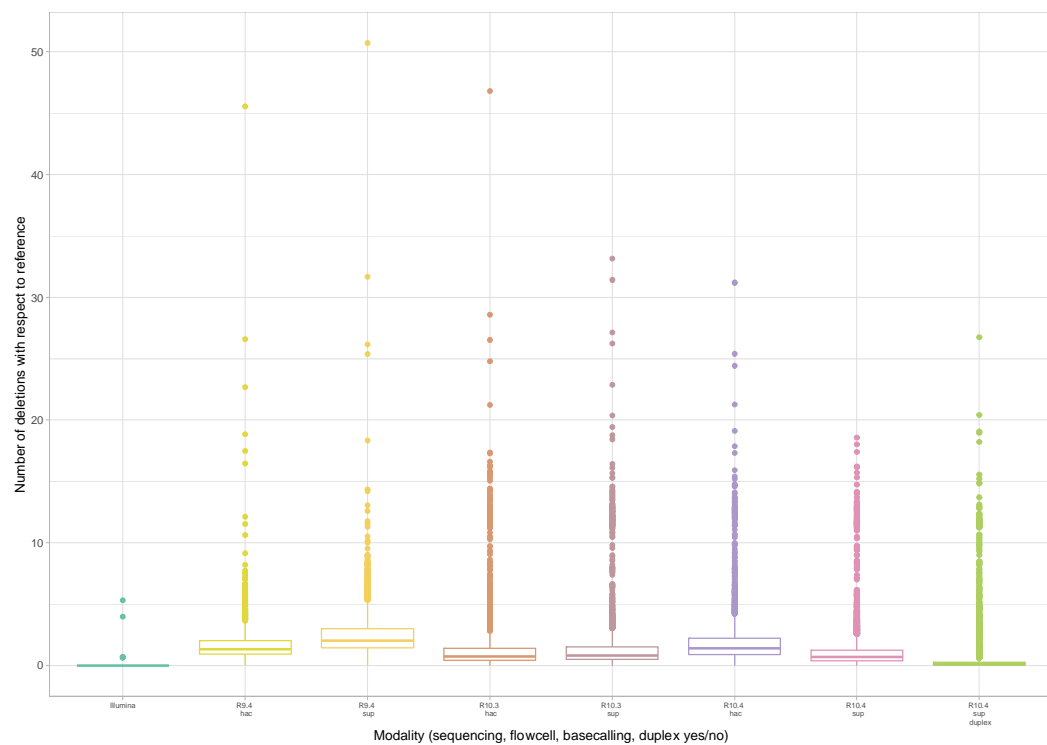
571 **A. Insertions**



572

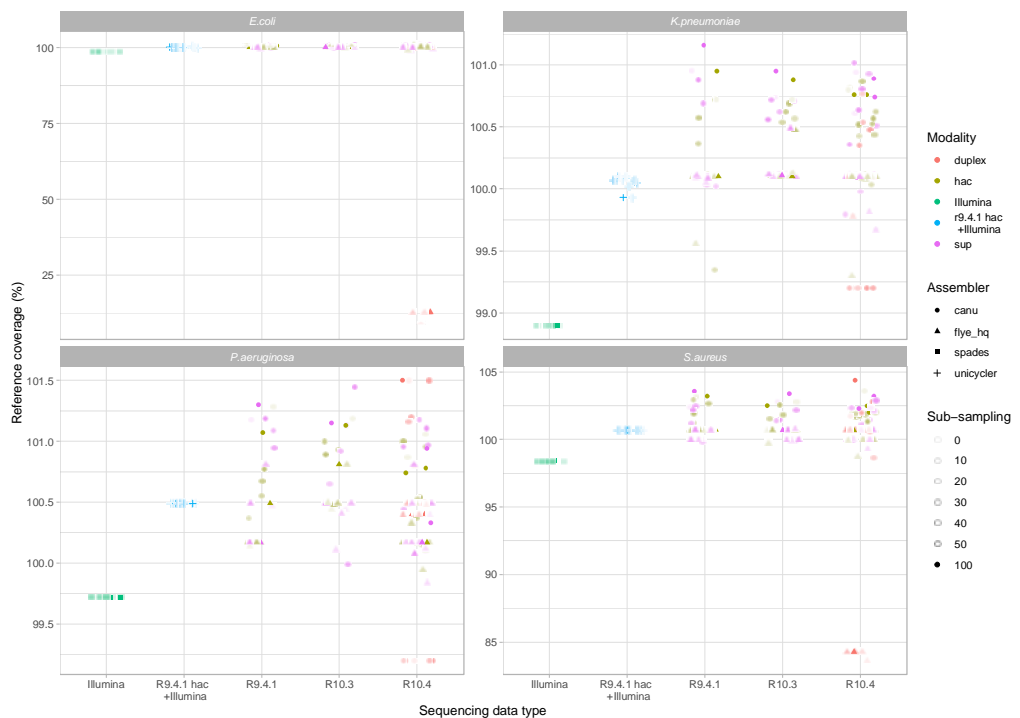
573 **B. Deletions**

574



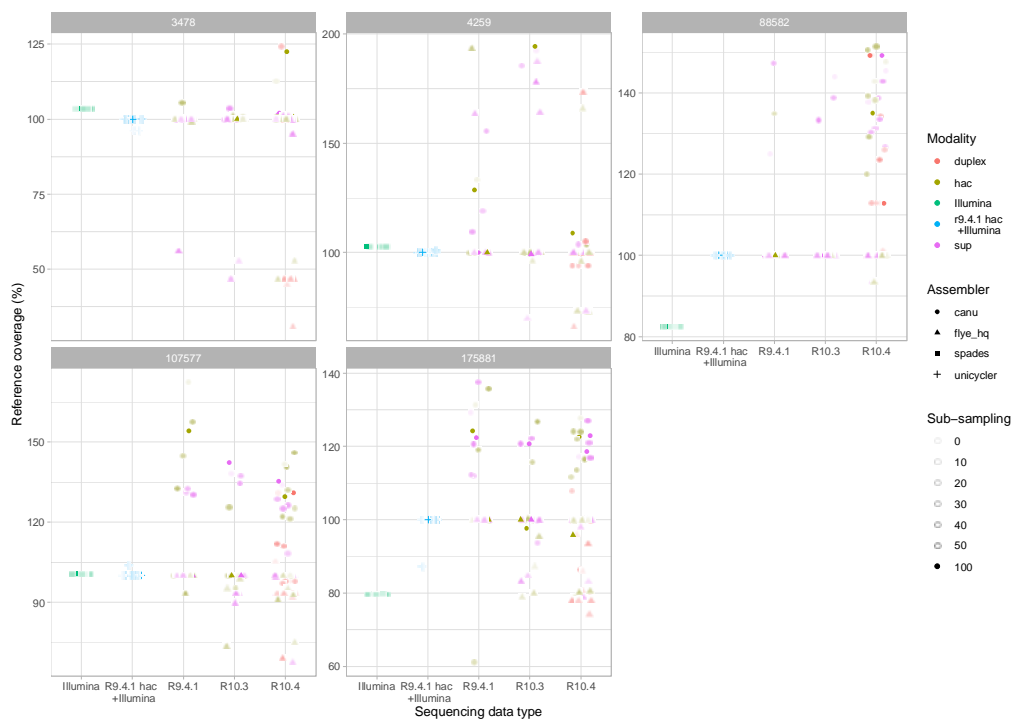
576 **Figure 5. Assembly reference coverage percentage (%) by sequencing modality,**
577 **assembler and species.** Panel A represents the data for chromosomes and panel B
578 evaluations for the five plasmids known to occur in the *K. pneumoniae* reference strain
579 (labeled by their lengths in bp).

580 **A. Chromosomes**



581

582 **B. Plasmids**

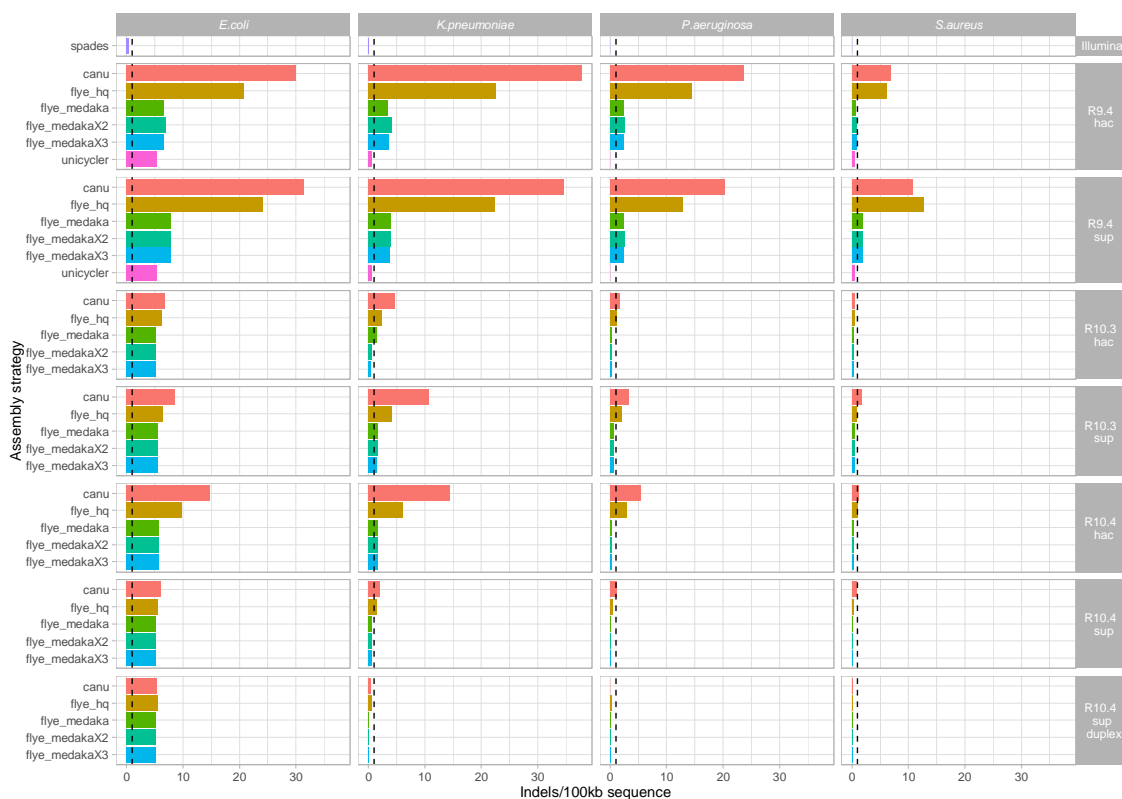


584 **Figure 6. Assembly accuracy by sequencing modality, assembly strategy and species.**

585 Accuracy evaluated on the basis of contig comparisons to Illumina-corrected references
586 using dnadiff, for (A) Indels, and (B) SNPs. NB - SPAdes was only used on Illumina data,
587 and Unicycler hybrid assembly was only performed on R9.4.1+Illumina data. For R10.4, data
588 presented are those from unplexed runs. Dashed black vertical line indicates a threshold of 1
589 error/100kb.

590

591 **A. Indel errors**



592

593

594 **B. Single nucleotide-level errors**

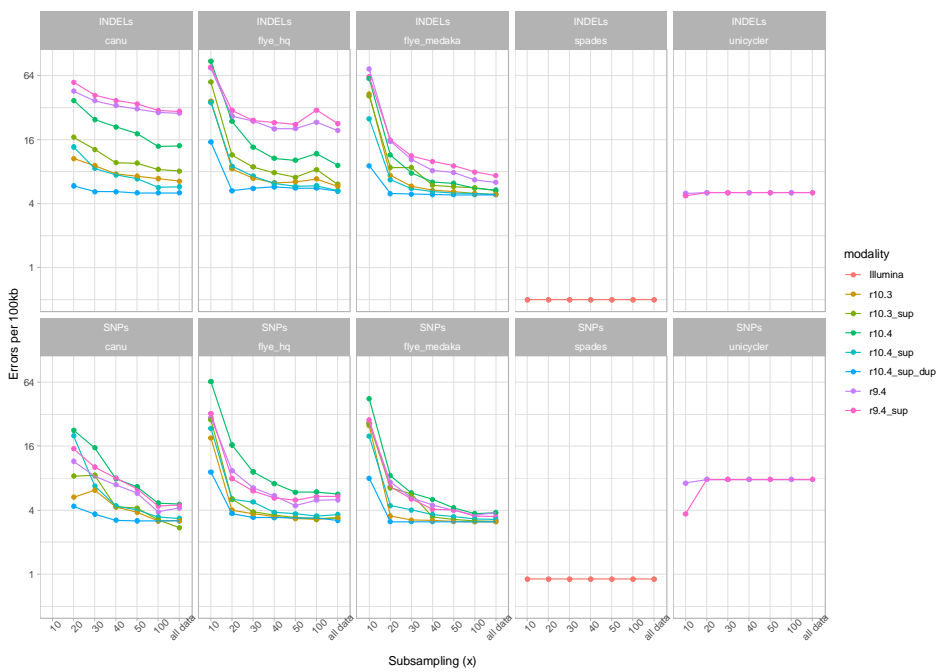
595



596

597 **Figure 7. Impact of subsampling of long-read datasets on assembly accuracy.**
598 Presented here by species for Indels (top panels), and SNPs (lower panels). For ease of
599 representation, only data for Flye assemblies polished with 1 round of Medaka are shown,
600 as the effects of additional polishing was shown to be marginal for most modalities (Fig.S6,
601 Table S7). Data for 10x long-read coverage is not omitted for Canu assemblies as this
602 coverage was considered too low for default settings and was unlikely to improve results.

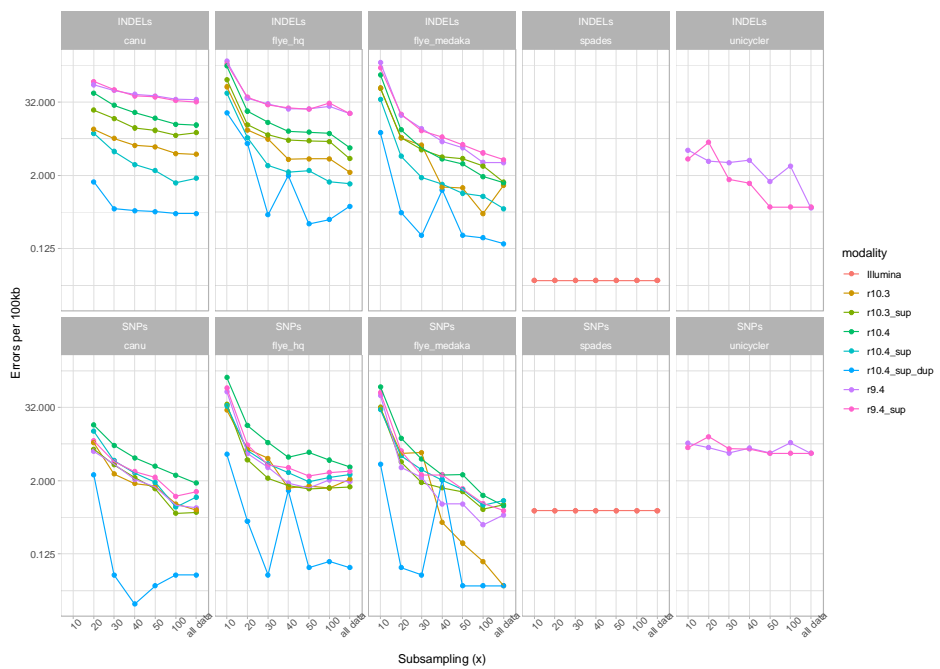
603 **A. *E. coli***



604

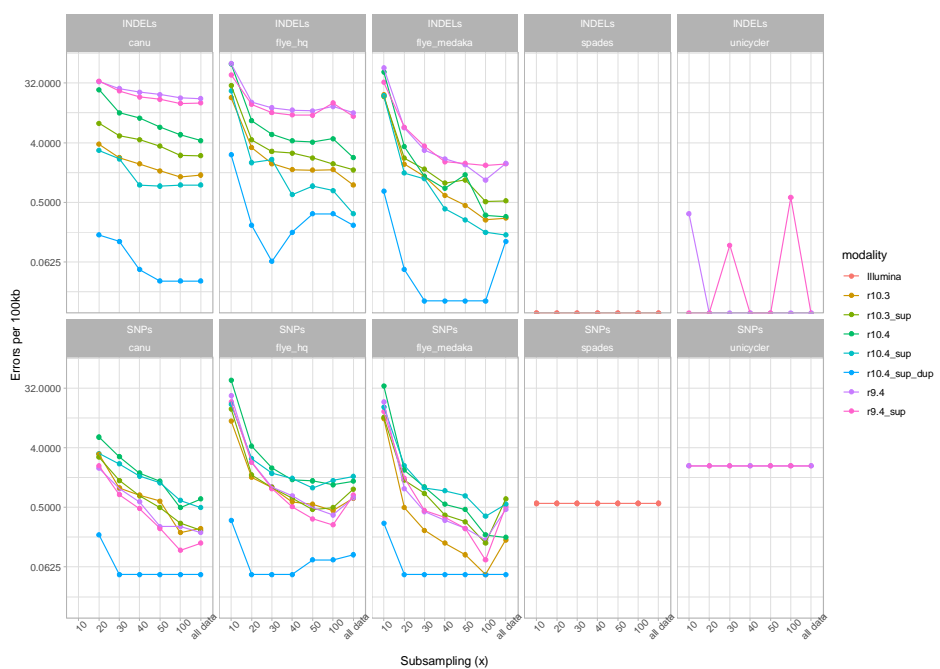
605 **B. *K. pneumoniae* (chromosome only)**

606



608

609 **C. P. aeruginosa**



611 **D. S. aureus**

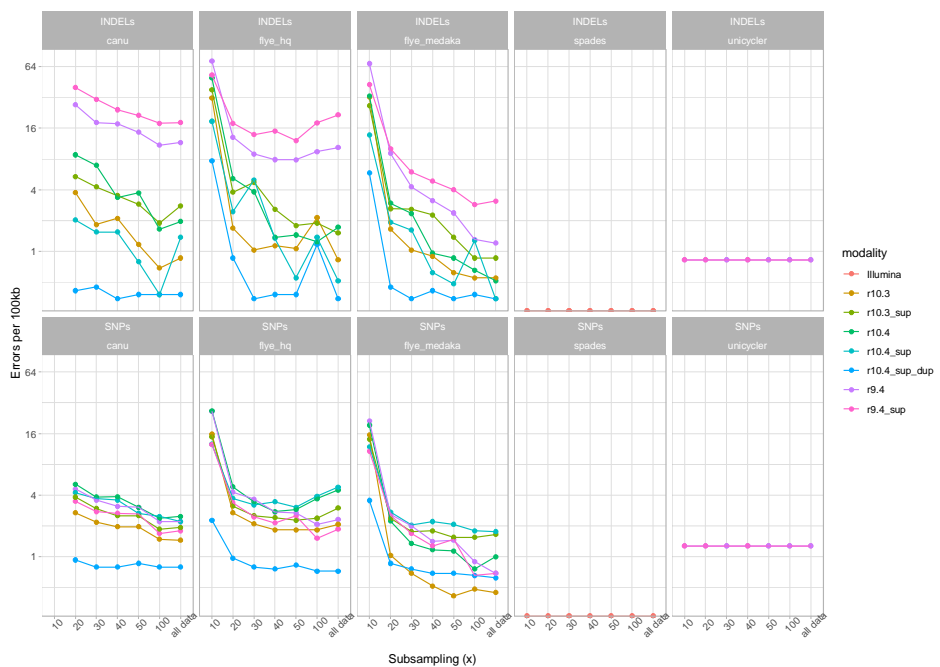


Figure 8. Coding sequence (CDS) recovery on the basis of exact CDS (amino acid sequence) matches with respect to the Prokka-annotated Illumina-corrected reference (chromosome+all plasmids for *K. pneumoniae*). Plot shows the percentage of reference coding sequences missed by each modality. For long-read data only Flye assemblies with one round of polishing with Medaka are shown; for R10.3 and R10.4 datasets these were from non-multiplexed evaluations (i.e. only single extracts per flowcell). For Unicycler, the assembly using R.9.4 hac+Illumina data is shown. The total number of coding sequences missed by each approach is shown as a number at the top of each bar.

